Article:

Aliyu, MM, Shan, J, Murphy, W orcid.org/0000-0002-7392-1527 et al. (4 more authors) (2019) Assessing the uniaxial compressive strength of extremely hard cryptocrystalline flint. International Journal of Rock Mechanics and Minings Sciences, 113. pp. 310-321. ISSN 1365-1609

https://doi.org/10.1016/j.ijrmms.2018.12.002

Assessing the uniaxial compressive strength of extremely hard cryptocrystalline flint

MM Aliyu[a], J. Shang[b,*], W Murphy[c], JA Lawrence[d], R Collier[c], F Kong[e], Z Zhao[b]

[a] Department of Civil Engineering Technology, Ramat Polytechnic, Maiduguri, Nigeria

[b] Nanyang Centre for Underground Space, School of Civil and Environmental Engineering, Nanyang Technological University, Singapore

[c] Institute of Applied Geosciences, School of Earth and Environment, University of Leeds, Leeds, United Kingdom

[d] Department of Civil and Environmental Engineering, Imperial College London, London, United Kingdom

[e] Research Center of Geotechnical and Structural Engineering, Shandong University, Jinan, China

Corresponding author: shangjunlongcsu@gmail.com; jlshang@ntu.edu.sg (J Shang)

To be appreared in the Int J Rock Mech Min Sci.
Received 27 September 2018
Accepted 04 December 2018

https://doi.org/10.1016/j.ijrmms.2018.12.002

Keywords: Flint; Uniaxial compressive strength; Empirical estimation; Drilling; TBM tunneling

Highlights

- An experimental study of the mechanical and mineralogical properties of cryptocrystalline flint.
- Assessment and development of UCS prediction models for the extremely strong cryptocrystalline flint.
- Validity study of the proposed models, and comparison between measured and estimated UCS.

Abstract

Cryptocrystalline flint is an extremely hard siliceous rock that is found in chalk formations. The chalk is frequently used as a host for underground rock caverns and tunnels in Europe and North America. A reliable estimation of the uniaxial compressive strength (UCS) of the extremely strong flint, with an average UCS of about 600 MPa will provide a scientific guidance for a proper engineering design, where flint is encountered, thereby avoiding project progress delay, litigation as well as economic consequences. Conventional UCS measurement using core samples is cumbersome for flint due to the extreme strength and hardness of the rock, for which the core sample preparation process is often extremely difficult. In this study, the UCS prediction models of flints collected from the North-West Europe were developed and the validity of the developed models was investigated. A series of laboratory index tests (comprising the three-point-bending, point load, ultrasonic velocity, density, Shore hardness and Cerchar Abrasivity tests) were perfomed. The index test results were correlated with the UCS values previously determined in the laboratory using both cylindrical and cuboidal specimens to develop the UCS prediction models. Regression analysis of the UCS and the index test results was then performed to evaluate for any potential correlations that can be applied to estimate UCS of the cryptocrystalline flint. Intensive validity and comparison studies were performed to assess the performance of the proposed UCS prediction models. This study showed that UCS of the tested flint is linearly correlated with its point load strength index, tensile strength and compressional velocity, and is

parabolically correlated with its density. The present study also demonstrated that only a couple of the previously developed empirical UCS models for estimating UCS are suitable for flint, which should be used with care.

1 Introduction

Flint is a siliceous, cryptocrystalline rock that forms in chalk formations which in recent decades are often used as a host for underground infrastructures like underground caverns, power houses and tunnels. Hosted by chalk, flint is extensively distributed in Europe and North America.[1] Flint is initially used as a manufacturing tool early days and now as one of the most critical engineering threats to drilling and tunneling in chalk-bearing flint, due to its extremely strong nature.

In the process of drilling or TBM tunneling, the existence of flint usually result in the deflecting of drill bits away from flint layers,[2] and more worse the severe wear of drill bits and TBM cutters, which can lead to the replacement of drill bits and cutters,[3] and in some cases the whole tunnel and TBM machine had to be redesigned.[4,5] Without a proper planning and design, experiencing these challenges will delay project progress,[6] thereby resulting in litigation as well as economic consequences.

Uniaxial compressive strength (UCS) is generally acknowledged to be often used in the current rock mass classification schemes (such as RMR and Q) and practical rock engineering applications.[7] It is generally recognized as one of the key rock properties, and as an initial step for a proper engineering design, to understand the UCS of flint. This parameter can be directly measured in the laboratory, following the ISRM standard[8], which relies on high-quality core samples and certified testing apparatus. One challenge is that the process of core sample preparation can be cumbersome, where extremely strong and hard rock such as the cryptocrystalline flint are encountered. As such, it is necessary to estimate and assess the UCS of flint using empirical methods.

Assessment of UCS through empirical methods (referring to index tests such as point load strength, ultrasonic and Cerchar abrasivity tests, etc.) has received significant attention since 1960s. One of the pioneering studies on this topic was reported by Deer and Miller[9], where five charts were proposed for estimating UCS of intact rock. The establishment of the charts was based on the results of a series of index tests on a total of 257 specimens collected from 27 localities in the United States.

Bieniawski[10] also assessed the applicability of using point load test results to estimate UCS and concluded that diametrical point load test was the most convenient and reliable in use; and this method was later recommended by the ISRM[11] for the measurement of point load index strength and the estimation of UCS.

After an extensive laboratory testing and multivariate statistical analysis, Ulusay et al.[12] proposed several polynomial equations for inferring UCS from the petrographic characteristics (i.e., texture, grain shape and size) and index properties (i.e., density, point load strength and porosity) of Litharenite sandstone in Turkey. Gokceoglu and Zorlu[13] and Kahraman et al.[14] reported linear relationships between UCS and the Brazilian tensile strength of various rocks.

Ultrasonic compressional and shear velocities have also been widely used in the estimation of UCS.[15-19] Kong and Shang[20] tested the validity of the point load and Schmidt hammer index tests in the estimation of UCS, by using a range of “standard” bricks, whereby the potential effects of lithological heterogeneity and grain size on results were removed. Those studies concluded that homogeneous rock samples should be used to get a reliable estimation results and point load tests exhibited a somewhat higher accuracy in the estimation of UCS.

Although hundreds of empirical equations for estimating UCS are available in literature, those relationships, however, are often rock-type and geological formation dependent. A considerable discrepancies (sometimes can be termed “error”) between estimated UCS and measured UCS can be expected when empirical equations derived from different rock types and formations were used (Kong and Shang[20]). Readily available and applicable UCS estimation models for characterising the extremely hard cryptocrystalline flint have not yet been developed. This hypothesis motivated the authors to experimentally explore prediction models for assessing the UCS of the flint, which has rarely been investigated and published.

The cryptocrystalline flint samples used in this study were collected from the North-West Europe, spanning from the United Kingdom, France to

Denmark. A series of index properties including point load strength index, three-point-bending tensile strength, ultrasonic velocities, density, Cerchar abrasivity index and Shore hardness, as well as UCS values of the collected samples were measured in the laboratory. The assessment and estimation of UCS of the cryptocrystalline flint using those index test results were performed by regression analysis and verification study was subsequently conducted. An intensive comparison study was presented by comparing the measured UCS and the estimated UCS using both the currently proposed and previously proposed UCS estimation models.

2 Sample collection and characterisation

2.1 Study sites, sample collection and characterisation

The flint samples used in the study were collected from the Upper Cretaceous Chalk formations within the North-West Europe, ranging from the Northern and Southern Provinces of the United Kingdom, the North Western France to the South Eastern Denmark (Fig. 1). Table 1 shows the nomenclatures and origins of the collected flint samples from the study sites. A detailed geological descriptions of the sites.

Some representative flint blocks are shown in Fig. 2. It can be seen that the samples exhibited different color (from light grey to dark brownish grey) which is the result of variation in mineral (calcite and silica) composition and degree of cementation as observed in Aliyu et al.[22]. Varying degrees of white carbonate inclusion (closed by the yellow dashed lines) can be noted from the appearance of the samples. Scanning Electron Microscope (SEM) examination of the flint samples demonstrated that these samples comprise homogenous cryptocrystalline quartz as the dominant mineral (87-99 %), with occasional calcite. Fig 2b shows that the flint sample collected from North Landing (BNLUK) exhibited a clear white crust (closed by the red dashed line) surrounding flint. The relationship between the white crust and flint is illustrated in Fig. 3, where a SEM image of the flint-crust boundary (see the thin section sample in Fig. 3a) is presented. A clear textural variation can be noted between the darker flint (Fig. 3b and 3c) and the more porous white crust (Fig. 3b and 3d). Another feature of flint is the presence sponge spicules and silicified micro-fossils.[23,24] This feature was also observed in the collected flint samples and is illustrated in Figs. 4c and 4d, where thin section photomicrographs of the flint sample SDFR (France) are presented. Figs 4a and 4b also reveal a void-filling phase dominated by euhedral mega quartz crystals surrounded by cryptocrystalline quartz.

2.2 Uniaxial compressive strength of the flint samples

The uniaxial compressive strengths of the flint samples (Fig. 2) were measured using both cylindrical and cuboidal specimens. In the preparation of the cylindrical specimens, the Richmond SR 2 radial brill was used, with a suitable speed of 1500 $Revmin^{-1}$,this was found to be the optimum drilling rate through a trial-and-error process . It has been observed from this coring process that the readily available core bits (normally used in the laboratory for regular rocks) were completely worn while coring 1-2 flint specimens (diameter 25 mm and length 60 mm). To resolve this issue, specially-manufactured core bits were used to drill the extremely strong cryptocrystalline flint.

Another problem encountered in the process of preparing cylindrical specimens from the BNLUK block was that it proved very difficult to prepare cores without breaking, which is mainly due to the presence of the white carbonate inclusions and micro-fractures (as shown in Fig. 2a). As an alternative, cuboidal specimens (breadth: 18-32 mm; height: 63-67 mm) were prepared for the BNLUK sample in accordance with the ASTM standard [25].

Ends of the cylindrical and cuboidal specimens were ground flat. The well-prepared flint specimens were then uniaxially compressed using the Denison loading machine (with a capacity of 2000 kN) at a loading rate of 0.5 $MPas^{-1}$. The axial stress was monitored by the machine, and the axial and lateral strains of the specimens during the compression were measured using 5 mm strain gauges.

Representative stress-strain curves of the tested specimens were shown in Fig. 5, from which Young's modulus and Poisson's ratio were calculated in accordance to the ISRM standard[8]. The mean UCS, Young's modulus and Poisson's ratio of the tested flint samples are shown in Table 2, with the associated standard deviations and the number of specimens tested included. As can be seen from the stress-strain curves (Fig. 5), the tested flint samples exhibited a typical linear deformation and failure occurred abruptly, without any evidence of a post failure record. The relatively higher standard deviation of UCS observed in Table 2 (Column 10) is related to the presence of carbonate inclusions in the samples (Fig. 2). The reported values of the Young's modulus and Poisson's ratio show small variations, which are however broadly consistent with Gercek[26] and Pabst and Gregorová[27]. Fig. 6 shows part of the flint specimens before and after the UCS test. Visual observations in the process of the UCS test revealed that axial splitting and brittle failure (leading to sharp and thin slabs, and small pieces, see Fig. 6d) dominated for the tested flint samples, which is often accompanied with catastrophic and explosive noise. Similar observations on flint UCS test were reported by Cumming[4].

3 Index tests and respective results

The term "index tests" used in the study refers to those simpler tests, whose results can potentially be used to correlate UCS of rock.[9,20,28-30] In the present study, several widely used index tests including three-point-bending, point load, ultrasonic velocity, density, Shore hardness and Cerchar Abrasivity tests were performed to explore and assess their feasibility for estimating the UCS of flint. A description of the process of each index test conducted in the study, and test results, are presented in this section.

To avoid coring and polishing (which is difficult for the strong and hard flint) as shown in Figs. 7a-7c, beam of flint specimens with a length to thickness ratio of more than 3 were prepared for the three-point-bending test, which follows Brook[31] and Fowell & Martin[32]. The test was carried out by placing each specimen on two ball bearings separated at various spans depending on the respective specimen dimensions. A concentrated load was applied at the center of each specimen until it fail in tension. In the meanwhile, the failure load was logged and used to calculate the tensile strength (indirect) of the flint. Corresponding results are shown in Table 2. Fig. 7d shows representative failure patterns of the beam specimens tested in the study.

The point load test was performed using a point load tester with a loading capacity of 56 kN and an accuracy of 0.05 N. The test was conducted on irregular blocks and lumps of flints (Figs. 8a, 8c and 8e), which is in accordance with the ISRM standard[8]. A steady load was applied on the specimens until failure, and the failure load was recorded and then used to calculate the standard point load index strength (i.e., $I_{s(50)}$, see also Table 2).

Figs. 8b, 8d and 8f present part of the failed flint specimens, from which it can be seen that several brittle fractures were always induced around the concentrated loading points.

ultrasonic pulse velocities following the ISRM suggested method[8], comprising compressional wave velocity (V_p) and shear wave velocity (V_s) of flint were measured using an Ergo Tech pulse generator (pulser 1-10). The flint specimens were placed between the transmitter and the receiver under a constant load of 0.2 kN. The load was then applied using the MAND uniaxial compression machine. Honey and a 0.1 mm thick lead foil were used to achieve an acceptable acoustic coupling between the specimens and the transducers. The transit time was measured and used to estimate the ultrasonic velocities (V_p and V_s). Table 2 shows the test results (Columns 3-4).

Cerchar abrasivity test originally introduced in Cerchar[33] has been widely used in the laboratory to assess the abrasivity of rocks, thereby, estimating TBM performance.[34-36] In this study, Cerchar abrasivity test was carried out on lumps of flint specimens, following the method used by Cerchar[33] to estimate the abrasiveness of flint, which translates to the drillability and cutterbility of the material. A standard Cerchar apparatus with a hard steel stylus of HRC 54-56 was used, and a static load of up to 90 N was applied on the stylus. Readings were taken from the worn pin under a microscope following a scratch (10 mm in length) on the samples. Results of the test were then interpreted as that used by Plinninger[37]; and the mean results for each sample are shown in Table 2 (Column 6).

Shore hardness (SH) reflects the hardness of rock, which is often used to evaluate the performance of drilling tools. Following the ISRM standard[8], the SH test was conducted on flint samples using the C-2 type SH testing machine. In the test, a 2.44 g diamond-tipped hammer was droppped freely on the specimen, and the rebound height was noted and recorded from the incorporated measuring scale. This procedure was then repeated fifty times on each specimen and readings were taken, while five highest as well as lowest readings were discarded in the data analysis. The average of the rebound heights from the remaining readings was taken as the shore hardness of the sample, which are shown in Table 2 (Column 5). The density of the flint samples was determined using the caliper method[8] and the mean results of each sample are shown in Table 2 (Column 2).

4 Assessing and development of UCS prediction models

4.1 Regression analysis

A series of regression analysis was performed to assess the potential correlations between UCS of flint and each index test result (i.e. ρ, V_p, V_s, SH, CAI, σ_t, and $I_{s(50)}$). In the analysis, different fitting functions such as linear, parabolic, exponential and lognormal were examined, and a R^2 value of no less than 0.5 was accepted in the study. Table 3 shows correlated equations for estimating UCS of the extremely strong and hard flint. It can be seen that three linear correlations were established, which include UCS - $I_{s(50)}$, UCS - σ_t, and UCS - V_p; and parabolic relation was found between UCS and density (ρ). No acceptable statistical correlations can be derived from V_s, SH, CAI to estimate UCS of flint, although these three index tests have been used to estimate UCS of various rocks such as marble[38], limestone and shale[39], and serpentinites[40].

4.2 Verification, comparison and discussion

To verify the capability of the proposed equations (Table 3), the estimated UCS values through the equations were assessed by comparing them with the measured UCS values as that used by Ng et al.[41] and Kong and Shang[20]. The comparison results are shown in Fig. 10, where most of the estimated data were close to the 100 % line, with an acceptable deviation of ~±20 % (i.e., within the region bounded by the 80 % and 120 % lines).

Additionally, the hypothesis mentioned in the Introduction (the empirical equations derived from other rocks may not be suitable for the estimation of the extremely hard flint) was tested in this section. Representative empirical relations (i.e. UCS - $I_{s(50)}$, UCS - σ_t, UCS - V_p and UCS - ρ) in literature were assembled (see the Appendix, Tables A1-A4). Those equations were respectively used to estimate UCS of the flint samples tested in the study. The estimated UCS values were compared with both the measured UCS and the estimated results via the equations proposed in the study. Fig 11a shows a comparison between the measured UCS (black dots) and the estimated UCS using the point load strength index ($I_{s(50)}$). It is noted that the scattered seven data points for each group (column) is related to the seven different sample sites, which corresponds to BNLUK, SESUK, BLSUK, SDFR, LMFR, TSDK and TMDK, respectively (from the top to the bottom). Box charts are also included in Fig 11a to graphically reflect some key values (i.e. mean, median, interquartile range, and maximum and minimum values) of the data from the statistics point of view. Mean value was used to assess the closeness of the data between each group.

As shown in Fig 11a, considerable discrepancies can be seen between the estimations (through $I_{s(50)}$) and the measured values, with a maximum overestimation of 54.9 % and a maximum underestimation of up to 65.3 %. Such huge differences can be treated as an “error” in practical rock engineering when some of the equations (for example that proposed by Tsiambaos and Sabatakakis[49]) were used to estimate the UCS of flint. Only a small part of the equations including those proposed by Singh[28], Ulusay et al.[12], Palchik and Hatzor[50], Basu and Aydin[52], Karaman et al.[58], Kong and Shang[20], as well as the one proposed in the present study (UCS=17.6 $I_{s(50)}$+13.5) gave an acceptable estimation of the UCS of flint. This phenomenon indicates that not all of the previously proposed UCS – $I_{s(50)}$ equations are unsuitable for the estimation of UCS of flints. The reason underlying this phenomenon is still not clear, as many geological and geographic factors, as well as diagenetic process may affect the results. A further study is necessary to explore the main factors controlling the discrepancy, so that a unified model can be developed. The present study further demonstrated that the UCS - $I_{s(50)}$ model proposed in this study (Table 3) and the previously derived UCS - $I_{s(50)}$ model presenting a good performance (mentioned above) are suggested to be used in the UCS estimation of flints.

Figs 11b, 11c and 11d show comparisons between the measured UCS and the UCS estimated using the three-point-bending tensile strength (σ_t), compressional velocity (V_p) and density (ρ), respectively. Similarly, clear and unacceptable discrepancies can be observed, especially for some cases where the maximum underestimations can be up to 81.6 % (Fig. 11c) and 87.6 % (Fig. 11d). Also without exception, the presently proposed UCS – V_p and UCS – ρ equations provide reliable estimations (Figs. 11c and 11d). For the estimation of UCS of flint using UCS – σ_t, the relations proposed by Din and Rafiq[29] and Kahraman et al.[14] also exhibited a good performance, besides the equation proposed in this study (Table 3, Fig. 11b).

5 Summary and conclusions

In this study, a compressive experimental investigation was carried out to explore suitable empirical models for estimating UCS of the extremely strong cryptocrystalline flint, which is special and often embedded in chalk formations. The UCS values of the flint samples collected from the UK, France and Denmark were first measured using both cylindrical and cuboidal specimens. A series of index tests including three-point-bending test, point load strength, ultrasonic velocity, density, Shore hardness and Cerchar abrasivity tests were performed in the laboratory. Regression analysis of the UCS and index test results was performed to probe any potential correlation models that can be used to estimate the UCS of flint. After that, a validity study of the proposed equations was presented, followed by the presentation of a comparison and discussion.

The uniaxial compressive strength of the cryptocrystalline flint tested in this study is linearly correlated with its point load strength index ($I_{s(50)}$), indirect tensile strength (σ_t) and compressional velocity (V_p), and is parabolically correlated with density (ρ). However, no acceptable statistical relations can be obtained between UCS and results from Shore hardness test, Cerchar Abrasivity test and shear velocity test. The four proposed empirical equations in this study have been proofed effective, and are therefore, suggested for estimating UCS of the extremely hard flint.The present finding, thus, implies that quick estimate of UCS of flints can now be made using simpler and non-destructive tests, thereby saving time and by implication costs (in engineering projects in chalk with flints).

The present study also revealed that a couple of the previously derived empirical UCS models from other rocks could be used to predict the UCS of flints, but with much care.

References

1. Shepherd W. Flint: its origin, properties and uses. Transatlantic Arts; 1st edition; 1972: pp 256.

2. Hahn-Pedersen M. AP Møller and the Danish Oil: Denmark, J.H. Schultz Grafisk. 1999; pp 357.
3. Banner S. Development of Munroe regional medical center. Star Banner 6A, Ocala, Florida; 2001.
4. Cumming FC. Machine tunnelling in chalk with flint with particular reference to the mechanical properties of flint. Unpublished PhD thesis, University of Brighton, UK. 1999.
5. Mortimore RN. Chalk: a stratigraphy for all reasons. The Scott Simpson Lecture: Proceedings of the Ussher Society, Geosciences in South West England. 2001; 10(2):105-122.
6. Peterson MNA. Deep Sea Drilling Project Technical Report: Core bits Contract NSF C-482, University of California, San Diego. 1974: Retrieved from http://deepseadrilling.org/t_reports.htm.
7. Hu J, Shang J, Lei T. Rock mass quality evalution of underground engineering based on RS-TOPSIS method. J Cent South Univ. 2012; 43(11): 4412-4419.
8. ISRM. The complete ISRM suggested methods for rock characterization, testing and monitoring: 1974-2006: In Ulusay, R., & Hudson, J. A. (eds) Suggested methods prepared by the commission on testing methods, International Society for Rock Mechanics, Commission on Testing Methods (ISRM Turkish National Group), 2007.
9. Deere DU, Miller RP. Engineering classification and index properties for intact rock. Technical Report. AFWL-TR-65-116. A. F. Weapons Laboratory, Kirtland. 1966.
10. Bieniawski ZT. The point-load test in geotechnical practice. Eng Geol. 1975; 9(1): 1-11.
11. ISRM. Suggested method for determining point load strength. Int J Rock Mech Min Sci Geomech Abstr.1985; 22(2): 51-60.
12. Ulusay R, Türeli K, Ider MH. Prediction of engineering properties of a selected litharenite sandstone from its petrographic characteristics using correlation and multivariate statistical techniques. Eng Geol. 1994; 38(1-2): 135-157.

13. Gokceoglu C, Zorlu K. A fuzzy model to predict theunconfined compressive strength and modulus of elasticity of a problematic rock. Eng Appl Artif Intell. 2004; 17:61-72.
14. Kahraman S, Fener M, Kozman E. Predicting the Compressive and Tensile Strength of Rocks from Indentation Hardness Index. J South Afr Inst Min Metall. 2012; 112(5): 331-339.
15. Tuğrul A, Zarif I H. Correlation of mineralogical and textural characteristics with engineering properties of selected granitic rocks from Turkey. Eng Geol. 1999; 51(4): 303-317.
16. Kahraman S. Evaluation of simple methods for assessing the uniaxial compressive strength of rock. Int J Rock Mech Min Sci. 2001; 38(7): 981-994.
17. Yaşar E, Erdoğan Y. Correlating sound velocity with the density, compressive strength and young's modulus of carbonate rocks. Int J Rock Mech Min Sci. 2004; 41(5): 871-875.
18. Yagiz S. P-wave velocity test for assessment of geotechnical properties of some rock materials. Bull Mater Sci. 2011; 34(4): 947-953.
19. Najibi A R, Ghafoori M, Lashkaripour G R., Asef M R. Empirical relations between strength and static and dynamic elastic properties of Asmari and Sarvak limestones, two main oil reservoirs in Iran. J Petrol Sci Eng. 2015; 126: 78-82.
20. Kong F, Shang J. A validation study for the estimation of uniaxial compressive strength based on index tests. Rock Mech Rock Eng. 2018; 51(7): 2289-2297.
21. Aliyu MM. The origin and properties of flint in the Upper Cretaceous Chalk. PhD thesis, the University of Leeds, United Kingdom. 2016; pp 283.
22. Aliyu MM, Murphy W, Lawrence JA, Collier R. Engineering geological characterization of flints. Q J Eng Geol Hydrogeo. 2017; 50(2): 133-147.
23. Bromley R G, Ekdale A A. Trace fossil preservation in flint in the European chalk. J Paleontol. 1984; 58: 298-311.
24. Donovan SK, Fearnhead FE. Exceptional fidelity of preservation in a reworked fossil, Chalk drift, South London, England. Geol J. 2015; 50(1): 104-106.

25. ASTM. Standard test method for laboratory determination of pulse velocities and ultrasonic elastic constants of rock (D2845-00). West Conshohocken, American Society for Testing Materials, ASTM. 2000.
26. Gercek H. Poisson's ratio values for rocks. Int J Rock Mech Min Sci. 2007; 44(1): 1-13.
27. Pabst W, Gregorová E. Elastic properties of silica polymorphs–a review. Ceramics – Silikáty. 2013; 57(3): 167-184.
28. Singh DP. Determination of some engineering properties of weak rocks. In: Proceedings of the international symposium on weak rock, Tokyo. 1981; pp. 21-24.
29. Din F, Rafiq M. Correlation between compressive strength and tensile strength/index strength of some rocks of North-West Frontier Province (limestone and granite). Geol Bull. 1997; 30:183-193.
30. Sousa LMO, Suárez del Río L M, Calleja L, Ruiz de Argandoña VG , Rey AR. Influence of microfraetures and porosity on the physieo-meehanieal properties and weathering of ornamental granites. Eng Geol. 2005; 77:153-168.
31. Brook N. The measurement and estimation of basic rock strength. Comprehensive rock engineering, Pergamon Press. 1993; 3: 41-66.
32. Fowell RJ, Martin JA. Cutterbility Assessment of Paramoudra Flints. A report for AMEC Civil Engineering Limited/Southern Water Limited. Department of Mining and Mineral Engineering, University of Leeds, 1997.
33. Cerchar. Centre d´Études et des Recherches des Charbonages de France. The Cerchar abrasiveness index. Verneuil. 1986.
34. Suana M, Peters T. The Cerchar abrasivity index and its relation to rock mineralogy and petrography. Rock mechanics. 1982; 15(1): 1-8.
35. Fowell R J, Abu Bakar MZ. A review of the Cerchar and LCPC rock abrasivity measurement methods. In: 11th Congress of the International Society for Rock Mechanics, Second half century for rock mechanics, Lisbon. 2007; 1: 155-160.
36. Käsling H, Thuro K. Determining abrasivity of rock and soil in the laboratory. In: Williams AL, Pinches GM, Chin CY, Mcmorran TJ, Massey CI. Geologically Active: Proceedings of the 11th IAEG Congress. CRC Press, London. 2010; 1973-1980.

37. Plinninger RJ. Abrasiveness assessment for hard rock drilling. Geomech Tunnelling. 2008; 1(1): 38-46.
38. Deliormanlı AH. Cerchar abrasivity index (CAI) and its relation to strength and abrasion test methods for marble stones. Constr Build Mater. 2012; 30:16-21.
39. Shalabi FI, Cording EJ, Al-Hattamleh OH. Estimation of rock engineering properties using hardness tests. Eng Geol. 2007; 90(3-4): 138–147.
40. Diamantis K, Gartzos E, Migiros G. Study on uniaxial compressive strength, point load strength index, dynamic and physical properties of serpentinites from Central Greece: test results and empirical relations. Eng Geol. 2009; 108:199-207.
41. Ng IT, Yuen KV, Lau CH. Predictive model for uniaxial compressive strength for grade III granitic rocks from Macao. Eng Geol. 2015; 199: 28-37.
42. D'Andrea DV, Fisher RL, Fogelson DE. Prediction of compression strength from other rock properties. Colo Sch Min Q. 1964; 59(4b): 623-640.
43. Broch E. Estimation of strength anisotropy using the point-load test. Int J Rock Mech Min Sci. 1983; 20:181-187.
44. Bieniawski ZT. The point-load test in geotechnical practice. Eng Geol. 1975; 9(1): 1-11.
45. Hoek E. Rock mechanics laboratory testing in the context of a consulting engineering organization. Int J Rock Mech Min Sci. 1977; 14: 93-101.
46. Cargill JS, Shakoor A. Evaluation of empirical methods for measuring the uniaxial strength of rock. Int J Rock Mech Min Sci Geomech Abstr. 1990; 27(6): 495-503.
47. Smith HJ. The point load test for weak rock in dredging applications. Int J Rock Mech Min Sci. 1997; 34: 295.e1–295.e13.
48. Hawkins AB. Aspects of rock strength. Bull Eng Geol Environ. 1998; 57:17-30.
49. Tsiambaos G, Sabatakakis N. Considerations on strength of intact sedimentary rocks. Eng Geol. 2004; 72(3-4): 261-273.
50. Palchik V, Hatzor YH. The influence of porosity on tensile and compressive strength of porous chalks. Rock Mech Rock Eng. 2004; 37(4): 331-341.

51. Fener M, Kahraman S, Bilgil A, Gunaydin O. A comparative evaluation of indirect methods to estimate the compressive strength of rocks. Rock Mech Rock Eng. 2005; 38(4): 329-343.
52. Basu A, Aydin A. Predicting uniaxial compressive strength by point load test: significance of cone penetration. Rock Mech Rock Eng. 2006; 39(5): 483-490.
53. Yilmaz I, Yuksek G. Prediction of the strength and elasticity modulus of gypsum using multiple regression, ANN, and ANFIS models. Int J Rock Mech Min Sci. 2009; 46: 803-810.
54. Basu A, Kamran M. Point load test on schistose rocks and its applicability in predicting uniaxial compressive strength. Int J Rock Mech Min Sci. 2010; 47(5):823-828.
55. Heidari M, Khanlari G R, Mehdi Torabi Kaveh, Kargarian S. Predicting the uniaxial compressive and tensile strengths of gypsum rock by point load testing. Rock Mech Rock Eng. 2012; 45: 265-273.
56. Kohno M, Maeda H. Relationship between point load strength index and uniaxial compressive strength of hydrothermally altered soft rocks. Int J Rock Mech Min Sci. 2012; 50(2):147-157.
57. Singh TN, Kainthola A, Venkatesh A. Correlation between point load index and uniaxial compressive strength for different rock types. Rock Mech Rock Eng. 2012; 45(2): 259-264.
58. Karaman K, Kesimal A, Ersoy H. A comparative assessment of indirect methods for estimating the uniaxial compressive and tensile strength of rocks. Arab J Geosci. 2015; 8:2393-2403.
59. Altindag R, Guney A. Predicting the relationships between brittleness and mechanical properties (UCS, TS and SH) of rocks. Sci Res Essays. 2010; 5(16): 2107-2118.
60. Nazir R, Momeni E Armaghani DJ, Amin MFM. Correlation between unconfined compressive strength and indirect tensile strength of limestone rock samples. Electron J Geotech Eng. 2013; 18:1737-1746.
61. Mohamad ET, Armaghani DJ, Momeni E. Prediction of the unconfined compressive strength of soft rocks: a pso-based ann approach. Bull Eng Geol Environ. 2015; 74(3): 745-757.

62. Çobanğlu İ, Çelik SB. Estimation of uniaxial compressive strength from point load strength, Schmidt hardness and P-wave velocity. Bull Eng Geol Environ. 2008; 67(4):491-498.
63. Sharma PK, Singh TN. A correlation between P-wave velocity, impact strength index, slake durability index and uniaxial compressive strength. Bull Eng Geol Environ. 2008; 67:17-22.
64. Khandelwal M, Singh T N. Correlating static properties of coal measures rocks with p-wave velocity. Int J Coal Geol. 2009; 79:55-60.
65. Moradian Z A, Behnia M. Predicting the uniaxial compressive strength and static young's modulus of intact sedimentary rocks using the ultrasonic test. Int J Geomech; 2009; 9(1):14-19.
66. Khandelwal M. Correlating P-wave velocity with the physico-mechanical properties of different rocks. Pure Appl Geophys. 2013; 170(4): 507-514.
67. Yesiloglu-Gultekin N, Gokceoglu C, Sezer EA. Prediction of uniaxial compressive strength of granitic rocks by various nonlinear tools and comparison of their performances. Int J Rock Mech Min Sci. 2013; 62(9): 113-122.
68. Azimian A, Ajalloeian R, Fatehi L. An empirical correlation of Uniaxial Compressive Strength with P-wave velocity and point load strength index on Marly rocks using statistical method. Geotech Geol Eng. 2014; 32(1):205-214
69. Tiryaki B. Predicting intact rock strength for mechanical excavation using multivariate statistics, artificial neural networks, and regression trees. Eng Geol. 2008; 99(1): 55-60.
70. Gupta V. Non-destructive testing of some Higher Himalayan rocks in the Satluj Valley. Bull Eng Geol Environ. 2009; 68(3): 409-416.

Figures

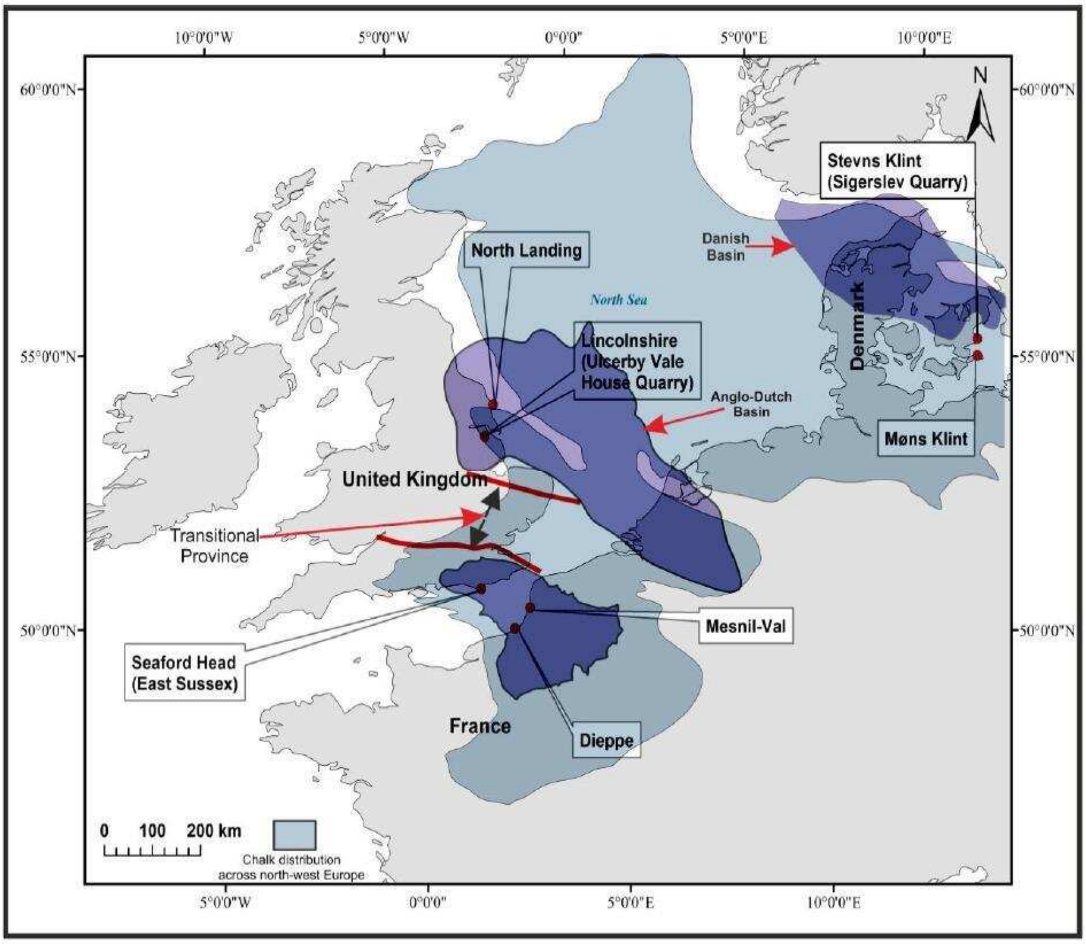

Fig. 1 Study sites indicated by the red dots. Adapted from Aliyu et al.[22]

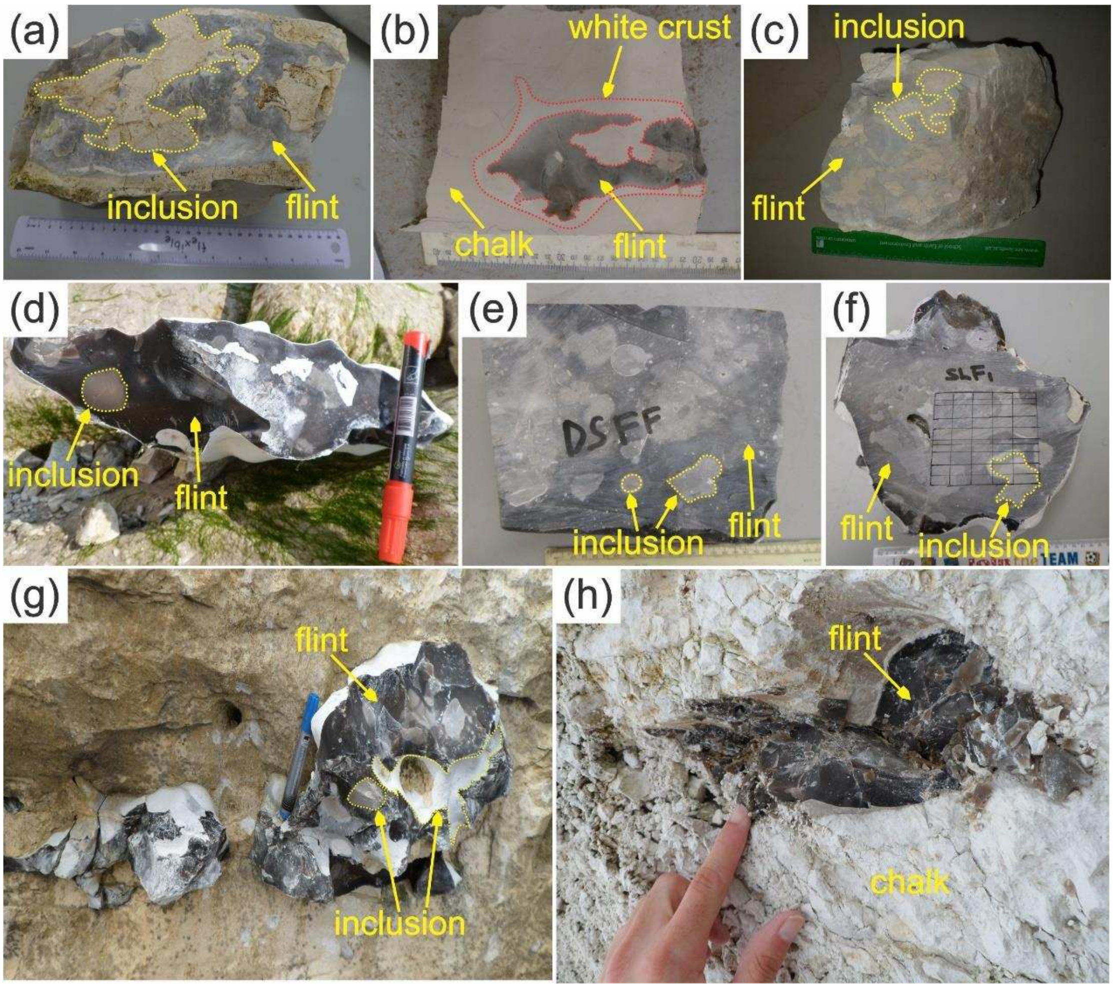

Fig. 2 Representative flint samples from the North-Western Europe. (a) and (b) BNLUK; (c) BLSUK; (d) SESUK; (e) SDFR; (f) LMFR; (g) TSDK and (f) TMDK. The carbonate inclusions and white crust (b) were closed by yellow and red dashed lines, respectively. See Table 1 for the nomenclature of the flint samples.

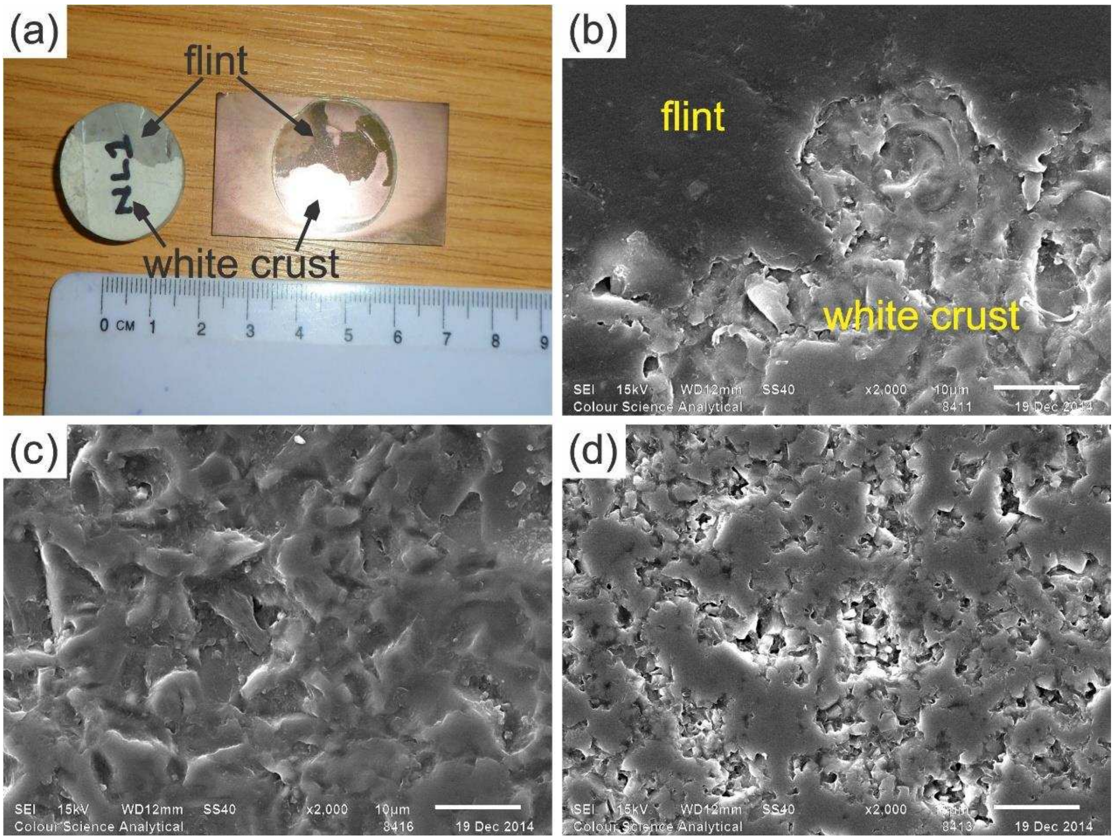

Fig. 3 (a) Samples used for the SEM analysis of the flint-crust boundary observed in Fig. 2b; (b) SEM of the flint-crust boundary from the North Landing flint (UK); (c) SEM of only the flint segment of the samples and (d) SEM of the crust segment of the sample. A clear textural variation can be observed between the darker flint and the more porous white crust.

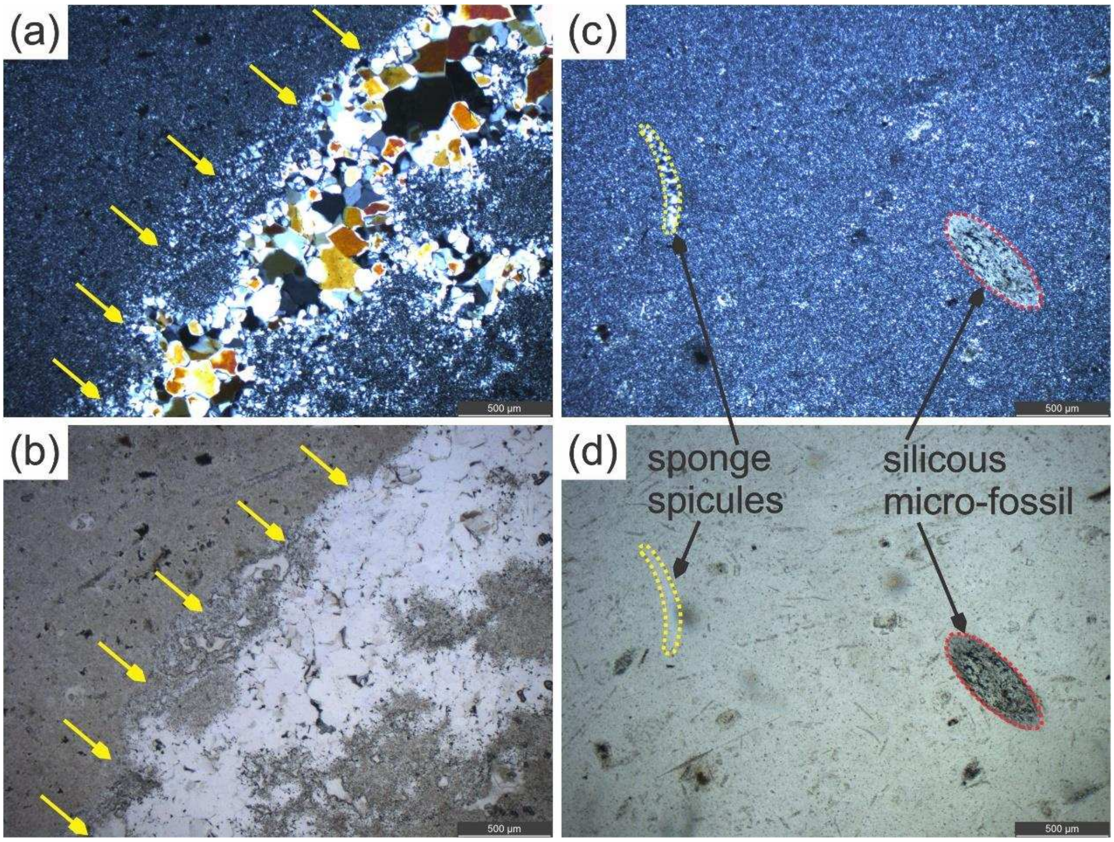

Fig. 4 Thin section photomicrographs of flint from the Seaford Chalk at Dieppe, France (SDFR, also see Fig. 2e. (a) and (c) Graphs observed under cross-polarized light; (b) and (d) are (a), and (c) presented under plane-polarized light. Note that Euhedral mega quartz crystals surrounded by cryptocrystalline quartz are shown by the yellow arrows ((a) and (b)). A sponge spicule and a siliceous micro-fossil were observed and closed by yellow and red dashed lines, respectively ((c) and (d)).

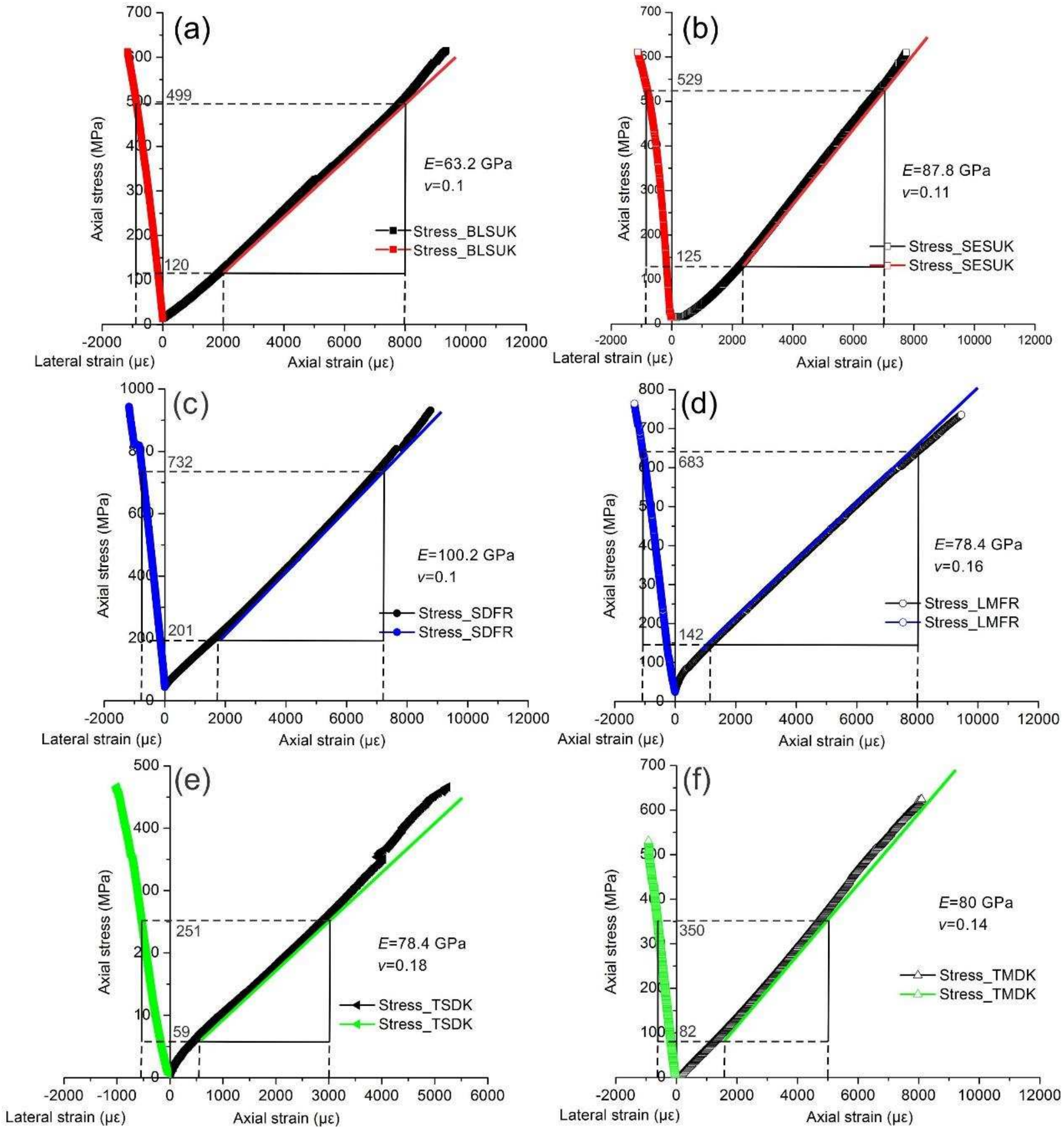

Fig. 5 Typical stress-strain curves for UCS tests on the tested flint samples. (a) BLSUK; (b) SESUK; (c) SDFR; (d) LMFR; (e) TSDK and (f) TMDK.

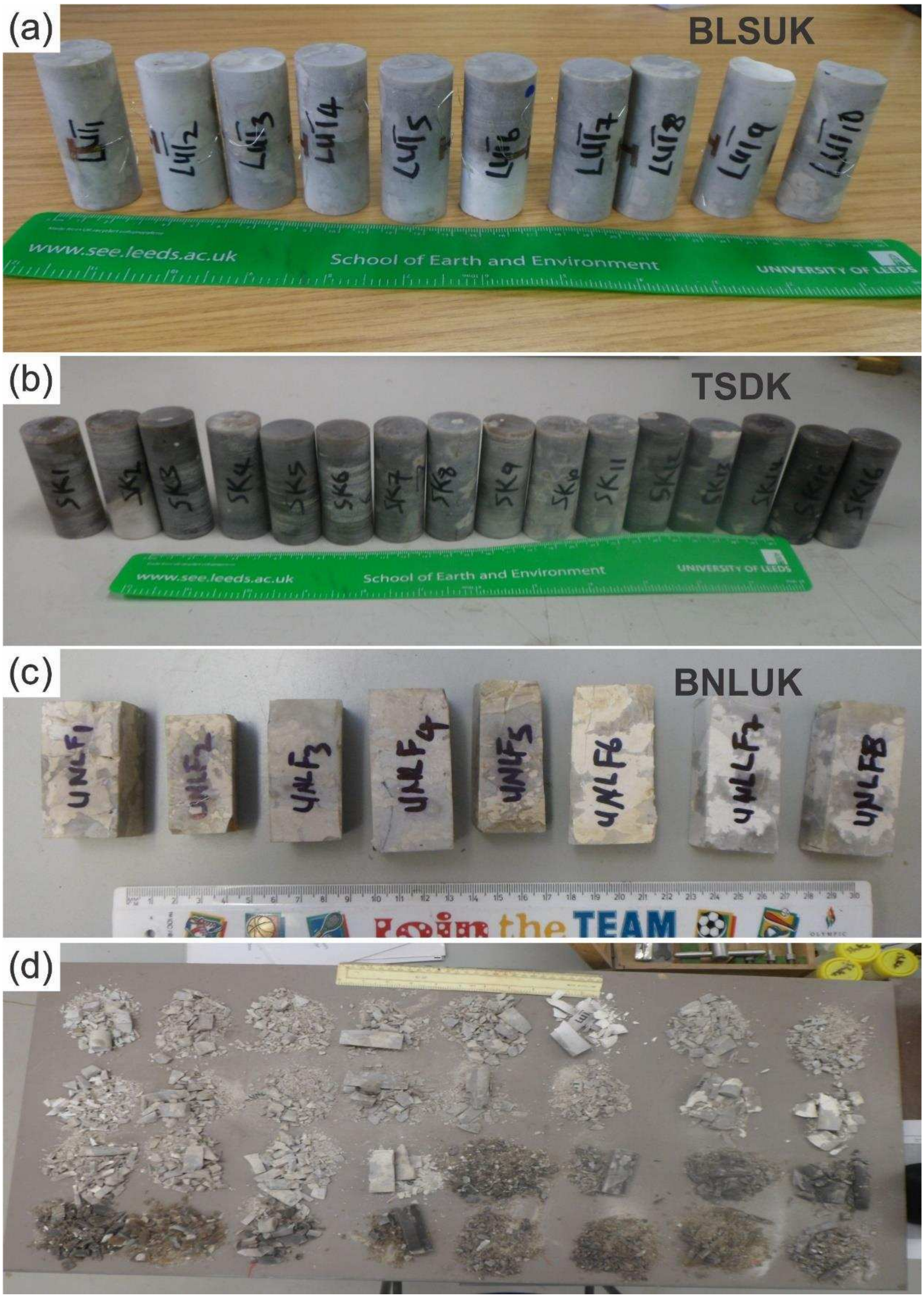

Fig. 6 Part of specimens before and after UCS test. Cylindrical specimens of BLSUK (a) and TSDK (b); (c) Cuboidal specimens of BNLUK and (d) failure patterns.

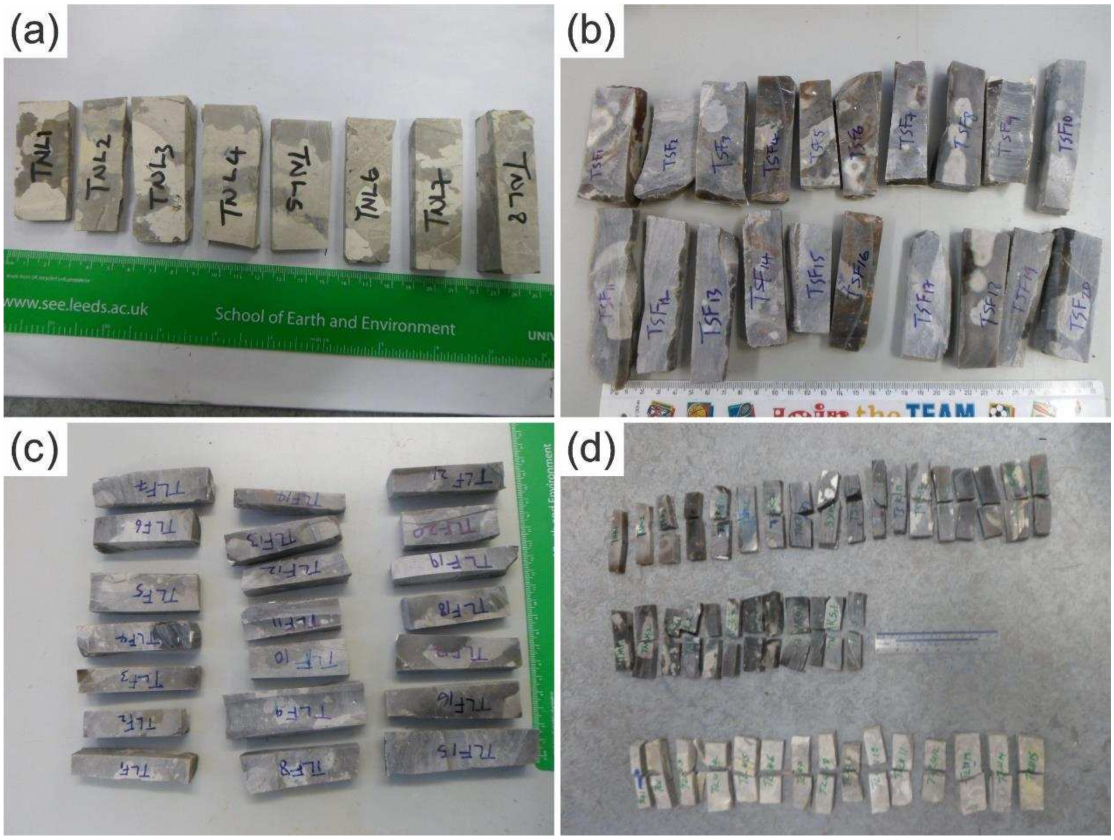

Fig. 7 Part of specimens before and after three-point-bending test. Beam specimens of BNLUK (a), SESUK (b) and LMFR (c); (d) Failure patterns.

Fig. 8 Part of specimens before and after point load test. (a) and (b) SDFR; (c) and (d) TMDK, and (e) and (f) TSDK.

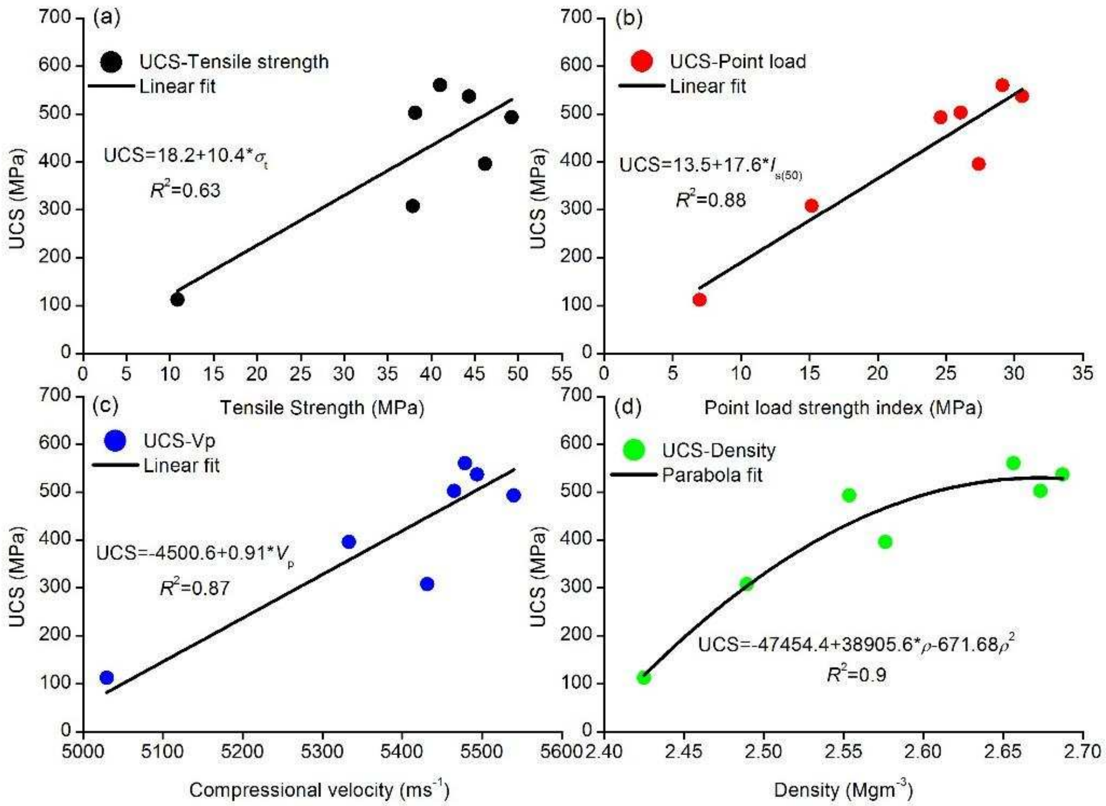

Fig. 9 Relationship between UCS of flint and index test results. (a) UCS vs. σ_t; (b) UCS vs. $I_{s(50)}$; (c) UCS vs. V_p and (d) UCS vs. ρ.

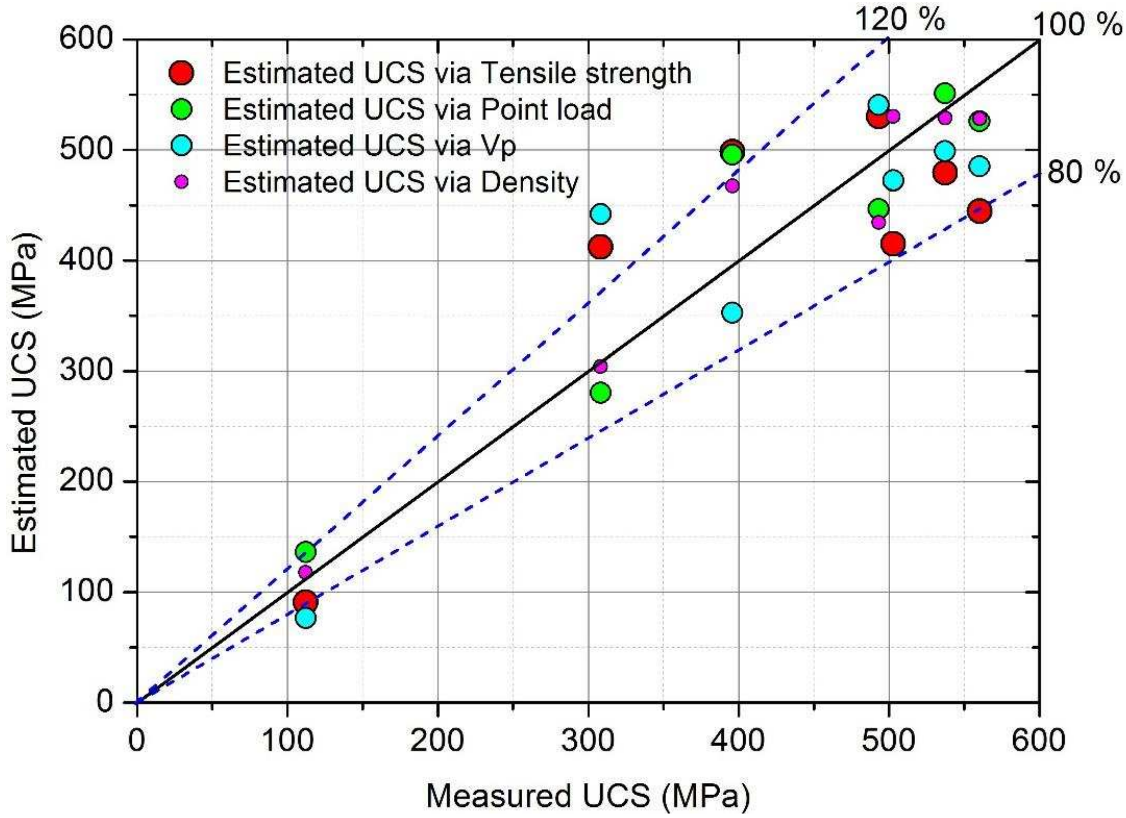

Fig. 10 Performance of the proposed equations (Table 3) in the UCS estimations. The 100 % line and the region bonded by the 80 % and 120 % lines are included for quantitative assessment.

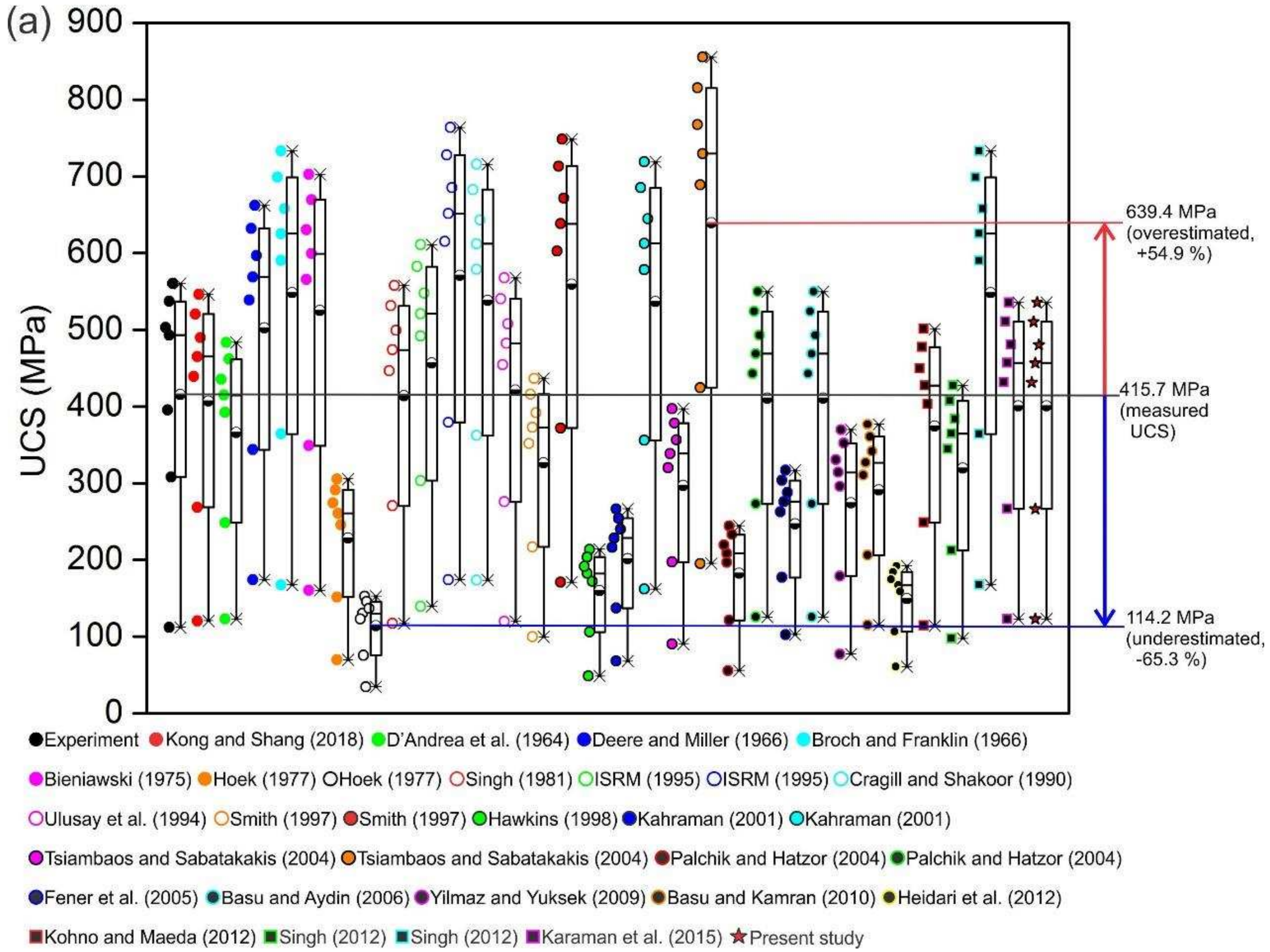
(a)
UCS (MPa)
900
800
700
600
500
400
300
200
100
0
639.4 MPa (overestimated, +54.9 %)
415.7 MPa (measured UCS)
114.2 MPa (underestimated, -65.3 %)
Experiment
Kong and Shang (2018)
D'Andrea et al. (1964)
Deere and Miller (1966)
Broch and Franklin (1966)
Bieniawski (1975)
Hoek (1977)
Hoek (1977)
Singh (1981)
ISRM (1995)
ISRM (1995)
Cragill and Shakoor (1990)
Ulusay et al. (1994)
Smith (1997)
Smith (1997)
Hawkins (1998)
Kahraman (2001)
Kahraman (2001)
Tsiambaos and Sabatakakis (2004)
Tsiambaos and Sabatakakis (2004)
Palchik and Hatzor (2004)
Palchik and Hatzor (2004)
Fener et al. (2005)
Basu and Aydin (2006)
Yilmaz and Yuksek (2009)
Basu and Kamran (2010)
Heidari et al. (2012)
Kohno and Maeda (2012)
Singh (2012)
Singh (2012)
Karaman et al. (2015)
Present study

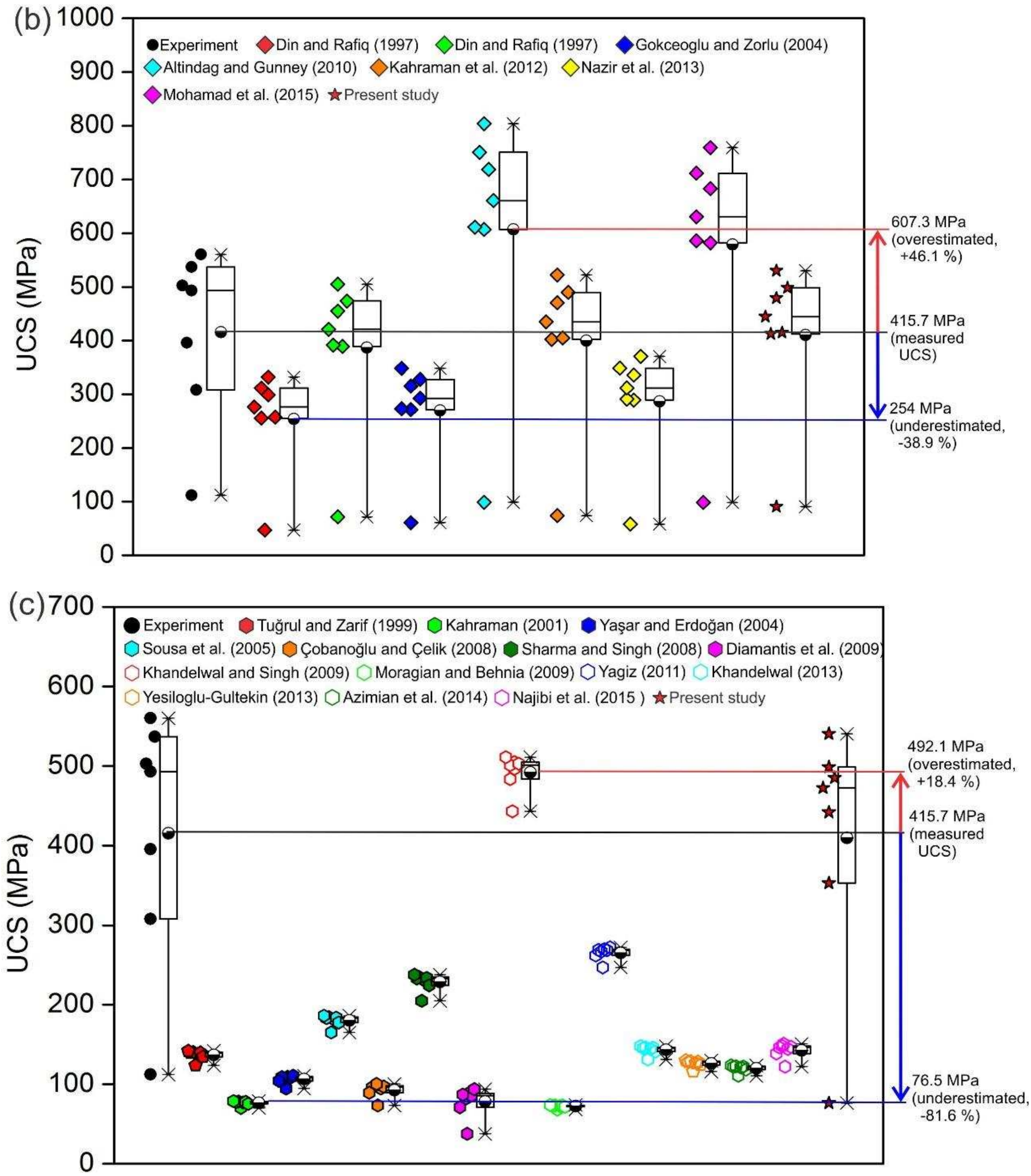

(b)
Experiment
Din and Rafiq (1997)
Din and Rafiq (1997)
Gokceoglu and Zorlu (2004)
Altindag and Gunney (2010)
Kahraman et al. (2012)
Nazir et al. (2013)
Mohamad et al. (2015)
Present study
UCS (MPa)
1000
900
800
700
600
500
400
300
200
100
0
607.3 MPa (overestimated, +46.1 %)
415.7 MPa (measured UCS)
254 MPa (underestimated, -38.9 %)
(c)
Experiment
Tuğrul and Zarif (1999)
Kahraman (2001)
Yaşar and Erdoğan (2004)
Sousa et al. (2005)
Çobanoğlu and Çelik (2008)
Sharma and Singh (2008)
Diamantis et al. (2009)
Khandelwal and Singh (2009)
Moragian and Behnia (2009)
Yagiz (2011)
Khandelwal (2013)
Yesiloglu-Gultekin (2013)
Azimian et al. (2014)
Najibi et al. (2015)
Present study
UCS (MPa)
700
600
500
400
300
200
100
0
492.1 MPa (overestimated, +18.4 %)
415.7 MPa (measured UCS)
76.5 MPa (underestimated, -81.6 %)

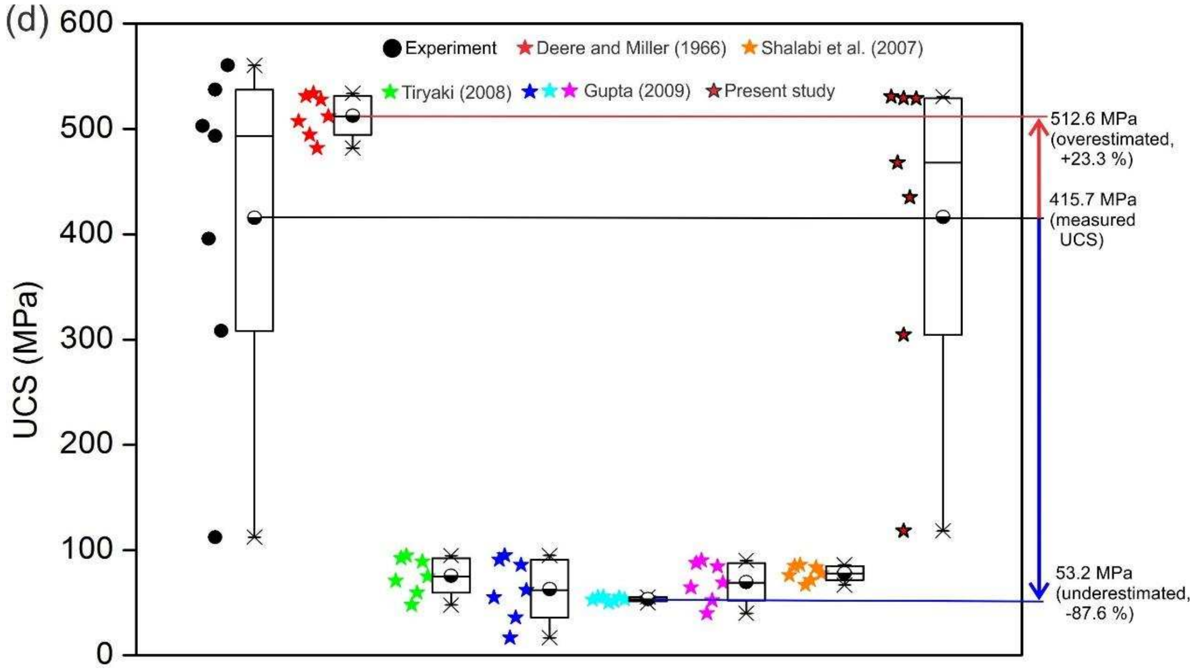

Fig. 11 Comparison between measured UCS and estimated UCS using previously proposed equations and presently proposed equations. (a) UCS vs. $I_{s(50)}$; (b) UCS vs. σ_t; (c) UCS vs. V_p and (d) UCS vs. ρ. Box charts are also included for assessing some key values of the data. See text for details.

Tables

Table 1 Nomenclature and origin of flint samples

Nomenclature of samples	Geological formation	Geographic location	Country
BNLUK	Burnham Chalk Formation	North Landing, Yorkshire	United Kingdom
SESUK	Seaford Chalk Formation	East Sussex	United Kingdom
BLSUK	Burnham Chalk Formation	Lincolnshire	United Kingdom
SDFR	Seaford Chalk Formation	Dieppe	France
LMFR	Lewes Chalk Formation	Mesnil-Val Plage	France
TSDK	Tor Chalk Formation	Stevns Klint	Denmark
TMDK	Tor Chalk Formation	Møns Klint	Denmark

Table 2 Properties and experimental results of flint samples.

Sample	Density, ρ (Mgm^{-3})	Compressional velocity, V_p (ms^{-1})	Shear velocity, V_s (ms^{-1})	Shore hardness	Cerchar Abrasivity index, CAI
BNLUK	2.43±0.12 (8)	5029.76±483.88 (8)	3530.77±307.30 (9)	109.48±5.80 (120)	3.39±0.53 (45)
SESUK	2.69±0.10 (20)	5493.96±95.93 (20)	3490.54±91.43 (16)	111.56±2.90 (320)	3.56±0.56 (52)
BLSUK	2.49±0.05 (20)	5431.47±306.81 (20)	3471.48±164.21 (40)	106.63±2.59 (86)	3.48±0.46 (50)
SDFR	2.67±0.13 (20)	5465.17±286.72 (20)	3571.27±166.95 (10)	108.45±2.32 (280)	3.66±0.47 (40)
LMFR	2.66±0.12 (20)	5479.06±223.43 (20)	3538.61±122.32 (10)	105.45±3.07 (80)	3.90±0.55 (40)
TSDK	2.55±0.01 (16)	5539.90±501.71 (16)	3609.96±229.23 (8)	111.76±2.22 (280)	3.59±0.35 (50)
TMDK	2.58±0.01 (5)	5333.51±210.55 (5)	3476.06±210.55 (5)	--	3.32±0.32 (50)

Sample	Tensile strength, σ_t (MPa)	Point load, $I_{s(50)}$ (MPa)	Uniaxial compressive strength, σ_c (MPa)	Young's modulus, E (GPa)	Poisson's ratio, V
BNLUK	6.97±2.63 (8)	6.97±3.85 (52)	112.19±71.04 (10)	--	--
SESUK	44.35±20.61 (49)	30.55±11.87 (82)	537.23±176.41 (20)	80.49±13.34 (20)	0.12±0.04 (20)
BLSUK	37.90±10.09 (12)	15.17±4.86 (17)	308.20±169.32 (16)	69.14±10.54 (10)	0.13±0.03 (10)
SDFR	38.15±13.65 (20)	26.06±8.93 (20)	502.88±150.35 (20)	85.13±16.12 (20)	0.12±0.03 (20)
LMFR	41.01±12.49 (20)	29.12±6.50 (20)	560.31±178.41 (20)	85.44±13.28 (20)	0.11±0.04 (20)
TSDK	49.24±5.67 (12)	24.60±9.17 (14)	493.18±222.13 (13)	74.01±25.01 (10)	0.14±0.05 (10)
TMDK	46.19±11.02 (6)	27.40±5.76 (7)	395.76±173.07 (5)	84.95±19.01 (6)	0.13±0.04 (6)

Note: The figure in the brackets represents the number of specimens / repetitions in each test.

Table 3 Proposed equations for estimating the uniaxial compressive strength of extremely hard flint.

Parameters	Equations	R^2
UCS, $I_{s(50)}$	UCS=17.6 $I_{s(50)}$+13.5	0.88
UCS, σ_t	UCS=10.4σ_t +18.2	0.63
UCS, ρ	UCS=-47454.4+35905.6ρ-6716.8ρ^2	0.90
UCS, V_p	UCS=0.91V_p-4500.6	0.80

Appendix

Table A1 Representative correlations between UCS and point load strength index ($I_{s(50)}$).

Equations	**Lithology**	**Number of samples (specimens) tested**	**References**
$UCS=15.3I_{s(50)}+16.3$	-	-	D'Andrea et al. (1964) [42]
$UCS=20.7I_{s(50)}+29.6$	Basalt, dolomite, sandstone, limestone, marble (US)	28 samples (257 specimens)	Deere and Miller (1966) [9]
$UCS=24I_{s(50)}$	-		Broch and Franklin (1972) [43]
$UCS=23I_{s(50)}$	-	-	Bieniawski (1975) [44]
$UCS=10I_{s(50)}$	Brittle rocks	-	Hoek (1977) [45]
$UCS=5I_{s(50)}$	Soft rocks	-	
$UCS=18.7I_{s(50)}-13.2$	Sandstone, sandy shale (India)	-	Singh (1981) [28]
$UCS=(20 - 25)I_{s(50)}$	-	-	ISRM (1985) [11]
$UCS=23I_{s(50)}+13$	Limestone, sandstone, marble (US)	14 samples (140 specimens)	Cargill and Shakoor (1990) [46]
$UCS=19I_{s(50)}-12.7$	Kozlu-Zonguldak sandstone (Turkey)	15 specimens	Ulusay et al. (1994) [12]
$UCS=14.3I_{s(50)}$	Biohermal lime rocks (US)	3 samples (57 specimens)	Smith (1997) [47]

$UCS=24.5I_{s(50)}$	Sandstone, limestone (US)	3 samples (75 specimens)	
$UCS=(7 - 68)I_{s(50)}$	Limestone, chalk, sandstone (UK)	-	Hawkins (1998) [48]
$UCS=8.41I_{s(50)}+9.51$	Limestone, sandstone, etc. (Turkey)	11 specimens	Kahraman (2001) [16]
$UCS=23.62I_{s(50)}-2.69$	Coal measure rocks-marl etc. (Turkey)	26 specimens	
$UCS=(13 - 28)I_{s(50)}$	Limestone, marly-limestone, sandstone, marlstone (Greece)	5 samples (20-93 specimens)	Tsiambaos and Sabatakakis (2004) [49]
$UCS=(8-18)I_{s(50)}$	Porous chalks	12-18 specimens	Palchik and Hatzor (2004) [50]
$UCS=9.08I_{s(50)}+39.32$	Basalt, granite, limestone, travertine, quartzite, marble, etc. (Turkey)	11 samples	Fener et al. (2005) [51]
$UCS=18I_{s(50)}$	Granitic rocks (Hong Kong, China)	40 specimens	Basu and Aydin (2006) [52]
$UCS=12.4I_{s(50)}-9.08$	Hafik Formation gypsum (Turkey)	121 specimens	Yilmaz and Yuksek (2009) [53]
$UCS=11.1I_{s(50)}+37.659$	Jaduguda uranium schist (India)	19 specimens	Basu and Kamran (2010) [54]
$UCS=5.575I_{s(50)}+21.92$	Gachsaran Formation gypsum (Iran)	15 specimens	Heidari et al. (2012) [55]
$UCS=16.4I_{s(50)}$	Hydrothermally altered volcaniclastic rocks (Japan)	44 specimens	Kohno and Maeda (2012) [56]
$UCS=(14 - 24)I_{s(50)}$	Gabbro, sandstone, limestone, shale, quartzite etc. (India)	11 samples (106 specimens)	Singh et al. (2012) [57]

UCS=17.5$I_{s(50)}$+1	Hamurkesen Formation basalt Berdiga Formation limestone (Turkey)	37 specimens	Karaman et al. (2015) [58]

Table A2 Representative correlations between UCS and tensile strength (σ_t)

Equations	**Lithology**	**Number of samples (specimens) tested**	**Methodology**	**References**
$UCS=(6.74 - 10.26)\sigma_t$	Granite and limestone	-	Brazilian test	Din and Rafiq (1997) [29]
$UCS=6.8\sigma_t + 13.5$	Andesite, agglomerate, greywacke, limestone, spilite, schist (Ankara basin, Turkey)	82 samples	Brazilian test	Gokceoglu and Zorlu (2004) [13]
$UCS=12.308\sigma_t^{1.0725}$	-	-	Brazilian test	Altindag and Guney (2010) [59]
$UCS=10.61\sigma_t$	Granite, basalt, sandstone, limestone, marble (Turkey)	46 samples	Brazilian test	Kahraman et al. (2012) [14]
$UCS=9.25\ \sigma_t^{0.947}$	Limestone	20 specimens	Brazilian test	Nazir et al. (2013) [60]
$UCS=15.361\sigma_t – 10.303$	Shale, old alluvium, iron pan (Nusajaya, Malaysia)	40 samples (160 specimens)	Brazilian test	Mohamad et al. (2015) [61]

Table A3 Representative correlations between UCS and P-wave velocity (V_p)

Equations	Lithology	Number of samples (specimens) tested	References
$UCS=0.03554V_p-55$	Granite, granodiorite (Turkey)	19 samples	Tuğrul and Zarif (1999) [15]
$UCS=9.95(10^{-3}V_p)^{1.21}$	Limestone, sandstone, coal measure rocks (Turkey)	37 specimens	Kahraman (2001) [16]
$UCS=0.0315V_p-63.7$	Limestone, dolomite, marble (Turkey)	13 specimens	Yaşar and Erdoğan (2004b) [17]
$UCS=0.004V_p^{1.247}$	Granite (Portugal)	9 samples	Sousa et al. (2005) [30]
$UCS=0.05293V_p-192.93$	Sandstone, limestone, cement motar (Antalya, Turkey)	150 specimens	Çobanğlu and Çelik (2008) [62]
$UCS=0.0642V_p-117.99$	Basalt, sandstone, phyllite, schist, coal, shaly rock	9 samples (48 specimens)	Sharma and Singh (2008) [63]
$UCS=0.11V_p-515.56$	Serpentinites (Greek)	32 samples	Diamantis et al. (2009) [40]
$UCS=0.1333V_p-227.19$	Sandstone, shale, coal (India)	12 samples	Khandelwal and Singh (2009) [64]
$UCS=165.058e^{(-4451/V_p)}$	Limestone, sandstone, marlstone (Iran)	64 samples	Moradian and Behnia (2009) [65]

$UCS=0.0494V_p-1.67$	Travertine, limestone, schist (Turkey)	9 samples (90 specimens)	Yagiz (2011) [18]
$UCS=0.033V_p-34.83$	Granite, sandstone, limestone, dolomite, marble (India)	13 samples	Khandelwal (2013) [66]
$UCS=0.027V_p-19.759$	Granite, granodiorite (Turkey)	6 samples (75 specimens)	Yesiloglu-Gultekin (2013) [67]
$UCS=0.026V_p-20.207$	Marly Formation rocks (Shiraz, Iran)	40 samples	Azimian et al. (2014) [8]
$UCS=3.67*(0.001V_p)^{2.14}$	Sarvak and Asmari limestone (Iran)	45 specimens	Najibi et al. (2015) [19]

Table A4 Representative correlations between UCS and density (ρ)

Equations	**Lithology**	**Number of samples (specimens) tested**	**References**
$UCS=(28812.5\rho-52.586)*0.0069$	Basalt, dolomite, sandstone, limestone, marble (US)	28 samples (257 specimens)	Deere and Miller (1966) [9]
$UCS=73\rho-110.32$	Dolomite (Chicago, US)	58 specimens	Shalabi et al. (2007) [39]
$UCS=178.33\rho-384.65$	-	-	Tiryaki (2008) [69]
$UCS=298\rho-706$ $UCS=21\rho-1$ $UCS=192\rho-425.8$	Granite, gneiss, quartzite, (India)	29 samples	Gupta (2009) [70]